Office of Naval Research
Department of the Navy
Contract N00014067-0094-0009

NONLINEAR EFFECTS IN THE COLLAPSE OF A NEARLY SPHERICAL CAVITY IN A LIQUID

by

Richard B. Chapman and Milton S. Plesset

Division of Engineering and Applied Science
California Institute of Technology
Pasadena, California

Report No. 85-51

July 1970

Nonlinear Effects in the Collapse of a Nearly Spherical Cavity in a Liquid*

by

Richard B. Chapman and Milton S. Plesset
California Institute of Technology

1. Introduction. A significant problem in the collapse of a spherical cavity in an infinite homogeneous liquid is the behavior of a distortion from complete spherical symmetry. The information presently available is based on a linearized perturbation analysis. When the analysis is made under the assumption of axial symmetry, the boundary of the cavity, r_s, may be written as

$$r_s(\theta, t) = R(t) + \sum_{n=2}^{\infty} a_n(t) P_n(\cos\theta) \quad , \tag{1}$$

where $P_n(\cos\theta)$ is the Legendre polynomial of degree n. In the perturbation theory it is supposed that

$$|a_n(t)| \ll R(t) \quad , \tag{2}$$

and the linearization uncouples the coefficients $a_n(t)$ and gives a mean radius $R(t)$ which develops in time independently of the distortion [1]. The solution to the general linearized equation for $a_n(t)$ was found by Plesset and Mitchell [2] for a bubble expanding or collapsing under a constant ambient pressure. This solution is expressed in terms of the hypergeometric function. It was found for a collapsing cavity that, as the mean radius approaches zero, $a_n(t)$ grows in magnitude like $R^{-\frac{1}{4}}$ and oscillates with increasing frequency. Even a small initial asymmetry will, therefore, become large for a sufficiently reduced cavity.

By use of the theory of Plesset and Mitchell, Naude and Ellis [3] analyzed their experimental observations of nearly hemispherical bubbles collapsing on a plane, solid wall. They observed that the distortions in the bubble shapes were primarily composed of the second harmonic with

*This study was supported by the Office of Naval Research

a small contribution from the fourth harmonic. No odd harmonics should be present, of course, because of the plane of symmetry. Naude and Ellis presented measured values for $a_2(t)$ and $a_4(t)$ over the first half of the collapse $(1.0 > R(t) > 0.5)$ and they observed that the values for $a_2(t)$ agreed with the predictions of the linearized perturbation solution. Since the contribution of the second harmonic was fairly large, Naude and Ellis found it necessary to determine the second order effect of $a_2(t)$ before close agreement on the theoretical predictions for $a_4(t)$ could be obtained.

An efficient numerical method has been developed to simulate the collapse of an initially spherical cavity near a solid wall [4], and this method is readily adapted to the simulation of the collapse in an infinite liquid of a nonspherical cavity with axial symmetry.

2. The Numerical Procedure. It is assumed that the flow is nonviscous and irrotational so that it may be described by a potential. It is assumed further that the effects of compressibility may be neglected. The collapse is driven by the difference between the ambient pressure, p_∞, and the pressure in the cavity, p_v. This pressure difference $\Delta p = p_\infty - p_v$ will be taken to be constant. When Δp is sufficiently large, surface tension may be neglected. Under these conditions the collapse of a cavity with a given initial shape with the mean initial radius R_o may be scaled to geometrically similar cavities. Velocities will scale with the factor $(\Delta p/\rho)^{\frac{1}{2}}$ where ρ is the liquid density.

The calculations are based on a series of small time steps. Before each step the potential problem is solved and the velocity is calculated at a large number of points representing the free surface of the cavity. If the time step Δt is sufficiently small, the velocities will remain relatively constant. The displacement of a free surface point with velocity $\vec{v}$ at the beginning of the time step is approximated by

$$\Delta\vec{x} = \vec{v}\Delta t \quad . \tag{3}$$

The change in the potential of the point at the free surface can be found from Bernoulli's equation

$$\frac{\partial \varphi}{\partial t} + \frac{1}{2} v^2 = \Delta p/\rho \quad .$$

The rate of change of the potential of a point moving on the free surface is

$$\frac{D\varphi}{Dt} = \frac{\partial \varphi}{\partial t} + v^2 \quad , \tag{5}$$

or

$$\frac{D\varphi}{Dt} = \Delta p/\rho + \frac{1}{2} v^2 \quad , \tag{6}$$

which gives the approximation

$$\Delta \varphi = \left(\Delta p/\rho + \frac{1}{2} v^2 \right) \Delta t \quad . \tag{7}$$

When the bubble starts from rest, the initial time step is treated differently. During the initial time step, the velocities are small compared with $(\Delta p/\rho)^{\frac{1}{2}}$. The displacements of the free surface points are small, and the potentials and velocities are nearly linear with time. Therefore the potential problem is solved for the initial time step with a uniform potential of $\Delta p/\rho$ over the initial cavity surface and the resulting velocity $\vec{V}$ is calculated at the free surface points. Then the velocity during the initial time step is

$$\vec{v} \simeq t \vec{V} \quad . \tag{8}$$

For the initial time step the displacement and potential of a point on the free surface is approximated by

$$\Delta \vec{x} = \frac{1}{2} (\Delta t_o)^2 \vec{V} \quad , \tag{9}$$

and

$$\varphi = \Delta t_o \left(\Delta p/\rho + \frac{1}{6} (\Delta t_o V)^2 \right) \quad . \tag{10}$$

A minor improvement in the method is to use the knowledge that the increase in velocity is nearly linear during the early stage of collapse to improve the accuracy for time steps throughout the early collapse

instead of only for the initial time step. The following approximation is used

$$\Delta\vec{x} = \frac{1}{2}\,\vec{v}\,[\,(t+\Delta t)^2 - t^2\,]\,t^{-1} \quad , \tag{11}$$

and

$$\Delta\varphi = (\Delta p/\rho)\Delta t + \frac{1}{6}\,v^2\,[\,(t+\Delta t)^3 - t^3\,]\,t^{-2} \quad . \tag{12}$$

3. Results of the Calculations

Two cases of initially nonspherical bubbles collapsing in a homogeneous liquid were simulated. For the first of these (Case A) the initial bubble shape, described by its radius,

$$r_s(\theta, 0) = 1 + \frac{1}{10}\,P_2(\cos\theta) \quad , \tag{13}$$

was roughly that of a prolate ellipsoid. The other case (Case B) had an oblate initial shape with a radius of

$$r_s(\theta, 0) = 1 - \frac{1}{10}\,P_2(\cos\theta) \quad . \tag{14}$$

The liquid was assumed to be initially at rest in both cases. A total of seventy-six time steps were used for Case A and eighty-six for Case B.

Bubble shapes for selected time steps from Cases A and B are shown superimposed in Figs. 1 and 2, respectively. Table I lists the time from the initiation of collapse for all of these shapes. The velocity of the bubble surface on the plane of symmetry and on the axis of metry is also listed for each shape. The times are given in units of $R_o(\rho/\Delta p)^{\frac{1}{2}}$. The velocities are given in meters/sec for

$$\frac{\Delta p}{\rho} = \frac{10^6\ \text{dynes/cm}^2}{1.0\ \text{g/cm}^3} \approx \frac{1\ \text{atm.}}{\text{density of water}} \quad . \tag{15}$$

Since it is of interest to compare the results of numerical simulation with the linear theory, a least squares fit was used for each cavity shape to determine the best values for the mean radius and the coefficients

TABLE I

Time Intervals from Initiation of Collapse, and Velocities of the Bubble Surface on the Plane of Symmetry and the Axis of Symmetry for Shapes Illustrated in Fig. 1 and Fig. 2.

Shapes of Fig. 1

Shape	Time	Velocity	
		On Axis of Symmetry	On Plane of Symmetry
A	.645	11 m/sec	8.7 m/sec
B	.775	20 m/sec	14 m/sec
C	.837	32 m/sec	20 m/sec
D	.871	46 m/sec	26 m/sec
E	.890	63 m/sec	33 m/sec
F	.901	76 m/sec	41 m/sec
G	.911	85 m/sec	54 m/sec
H	.918	93 m/sec	78 m/sec
I	.9225	102 m/sec	119 m/sec

Shapes of Fig. 2

Shape	Time	Velocity	
		On Axis of Symmetry	On Plane of Symmetry
A	.645	8.0 m/sec	11 m/sec
B	.775	12 m/sec	17 m/sec
C	.837	17 m/sec	27 m/sec
D	.879	23 m/sec	42 m/sec
E	.907	38 m/sec	77 m/sec
F	.918	64 m/sec	126 m/sec
G	.9216	85 m/sec	243 m/sec
H	.9221	91 m/sec	336 m/sec
I	.9224	95 m/sec	518 m/sec

in the expansion

$$r_s(\theta, t) = R(t) + \sum_{n=1}^{5} a_{2n}(t) P_{2n}(\cos\theta) \quad . \tag{16}$$

This fit was successful except for the last few time steps, when the bubble was highly distorted. Figures 3 and 4 show $a_2(t)$, $a_4(t)$, and $a_6(t)$ as function of R(t). For comparison $a_2(t)$ computed from the linear theory of Plesset and Mitchell is also included.

In Case A, the initial elongation of the bubble along its axis causes the velocity on the bubble surface to be greatest at the poles early in the collapse. This deformation eventually causes the formation of jets on the axis of symmetry, which have a velocity of about 100 m/sec under the conditions of Eq. (15) when they strike. Similarly, the velocity on the bubble surface is a maximum at the plane of symmetry in Case B, and the bubble assumes a "dumbbell" shape. As the center of the bubble in Case B constricts about the axis, the radial velocity near the plane of symmetry grows without limit. This unbounded rise in radial velocity is a result of the assumption of axial symmetry; a small initial distortion lacking axial symmetry would prevent it.

According to the linearized theory, $a_2(t)/a_2(0)$ should follow the same curve for both Case A and Case B, and all other coefficients should remain zero throughout the collapse. The nonlinear solution during the first part of collapse conforms more closely to linear theory than might be expected for an initial distortion of ten percent. During the final part of the collapse, the nonspherical terms in the bubble shape and velocity grow to the order of magnitude of the spherical terms, causing the higher harmonics to be excited. The behavior of $a_4(t)$ closely follows the second order results of Naude and Ellis (not shown here). Throughout the collapses $a_2(t)$ remains surprisingly close to the linear estimate. The theory of Plesset and Mitchell predicts that $a_2(t)$ will oscillate with increasing frequency as the mean radius approaches zero. The distortion in both cases is large enough, however, so that parts of the bubble strike each other before an entire oscillation can be completed.

5. Adjustment for Finite Time Steps

The chief source of error in these calculations is the use of finite time steps. A close estimate of this error can be made by computing the effect of the same time steps used in Cases A and B on bubbles satisfying the linearized equations.

In the linearized approximation to Cases A and B, the second harmonic is the only nonspherical term in the radius of the free boundary;

$$r_s(\theta, t) = R(t) + a(t)P_2(\cos\theta) \quad . \tag{17}$$

It is assumed, of course, that $|a(t)| \ll R(t)$. Also, to first order the potential on the free surface can be written as

$$\varphi[\, r_s(\theta, t), \theta, t] = A(t) + C(t)P_2(\cos\theta) \quad . \tag{18}$$

By an analysis similar to that of Reference [1] it is found that, in the linearized approximation,

$$\dot{R} = -\frac{A}{R} \quad , \tag{19}$$

$$\dot{a} = -\left(\frac{3C}{R} + \frac{Aa}{R^2}\right) \quad , \tag{20}$$

$$\dot{A} = \frac{\Delta p}{\rho} + \frac{1}{2}\frac{A^2}{R^2} \quad , \tag{21}$$

and

$$\dot{C} = \frac{A}{R}\left(\frac{3C}{R} + \frac{Aa}{R^2}\right) \quad . \tag{22}$$

Thus the linearized equivalent of Eq. (3) is

$$\Delta R = -\frac{A}{R}\Delta t \quad ; \qquad \Delta a = -\left(\frac{3C}{R} + \frac{Aa}{R^2}\right)\Delta t \quad ; \tag{22}$$

and the linearized equivalent of Eq. (7) is

$$\Delta A = \left(\frac{\Delta p}{\rho} + \frac{1}{2} \frac{A^2}{R^2} \right) \Delta t \quad ; \qquad \Delta C = \frac{A}{R} \left(\frac{3C}{R} + \frac{Aa}{R^2} \right) \Delta t \quad . \tag{24}$$

Linearized equivalents of Eqs. (9), (10), (11), and (12) are obvious.

The time steps used in Cases A and B were applied to these linearized equations to obtain an adjusted linearized solution. The difference between this adjusted linearized solution and the true linearized solution represents the error caused by the use of finite time steps. The adjusted linearized solution is shown with the true linearized solution and the second harmonic determined from the nonlinear solution in Fig. 5 for Case A and in Fig. 6 for Case B. It is seen that the second harmonic from the nonlinear solution is even closer to linear theory when the effect of finite time steps is taken into account.

The major nonlinear effect is the excitation of the higher harmonics. This nonlinear effect has an important influence on the jet in Case A as can be illustrated by a calculation using linearized theory for the speed on the axis of symmetry when the opposite jets strike. The result is about 193 m/s using the exact linearized solution and about 189 m/s using the linearized solution adjusted for the finite time steps used in Case A. The difference between these two values gives a measure of the error caused by the finite time steps. Both values are almost twice the observed jet speed in the nonlinear calculation. This difference reflects the large contributions from the higher order harmonics in the final stages of collapse.

Bibliography

1. M. S. Plesset, J. Appl. Phys. 25, 96 (1954).

2. M. S. Plesset and T. P. Mitchell, Quart. Appl. Math. 13, 439 (1956).

3. C. F. Naude and A. T. Ellis, J. Basic Eng. 83, 648 (1961).

4. M. S. Plesset and R. B. Chapman, in press.

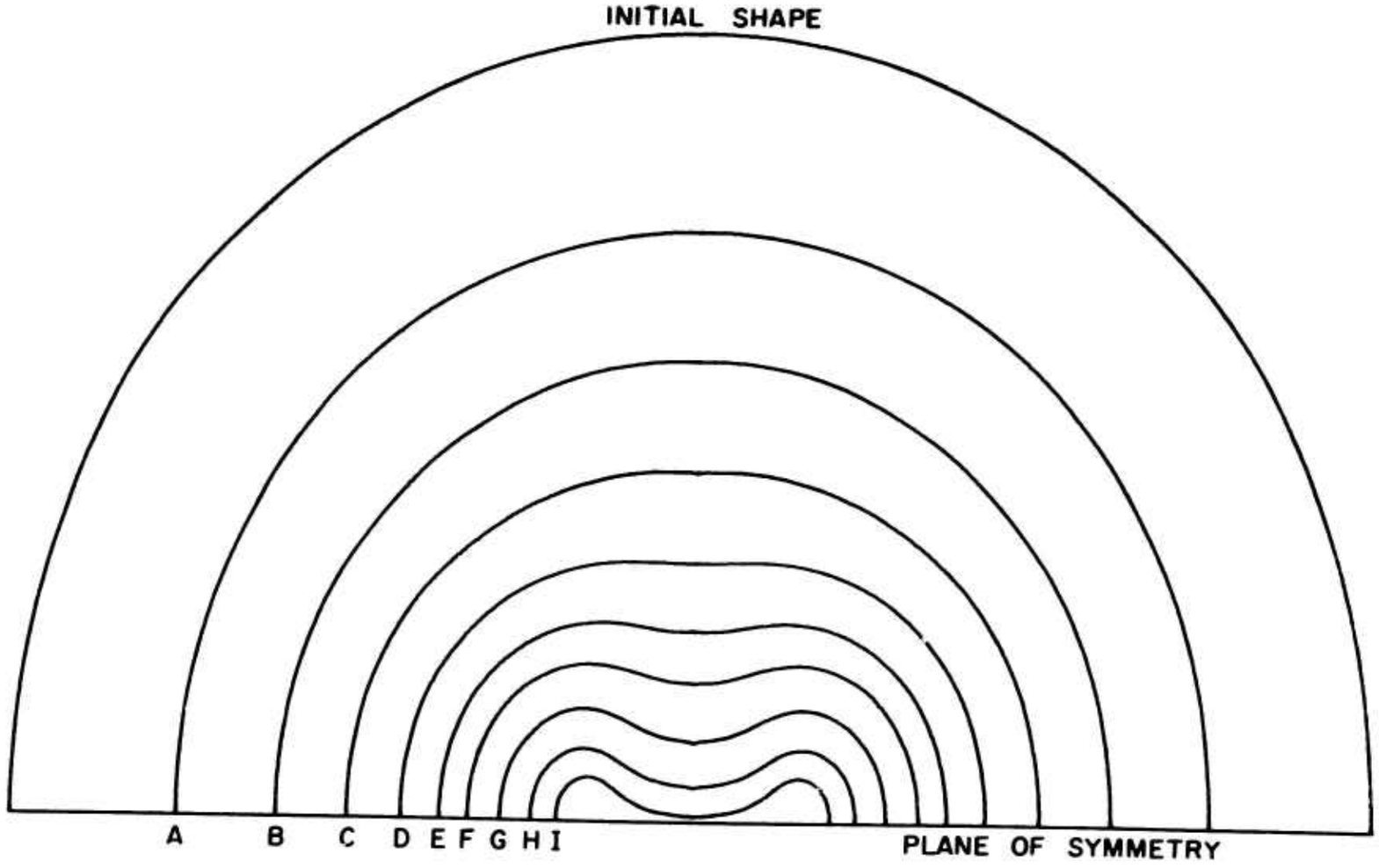

Fig. 1 Bubble Surfaces from Case A.

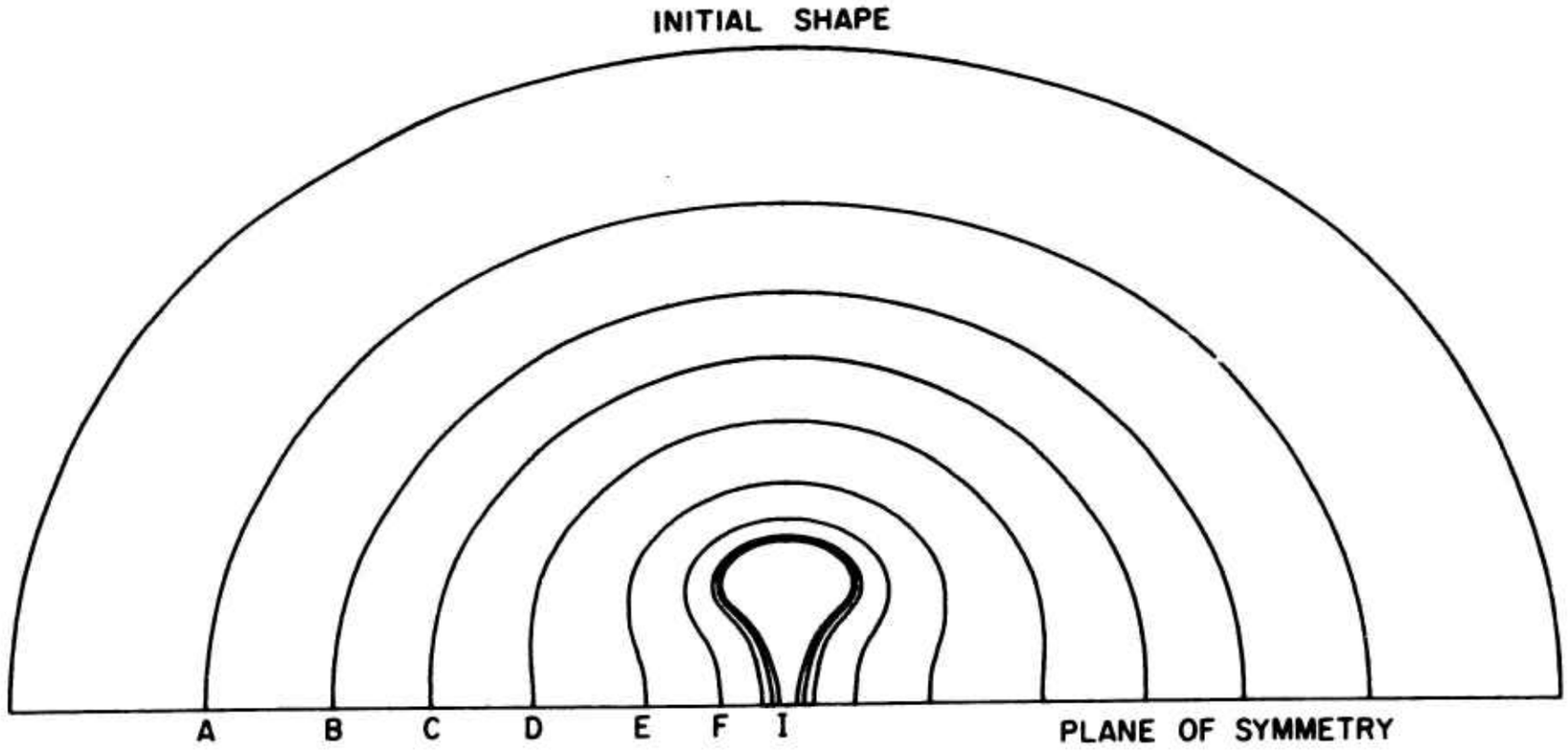

Fig. 2 Bubble Surfaces from Case B.

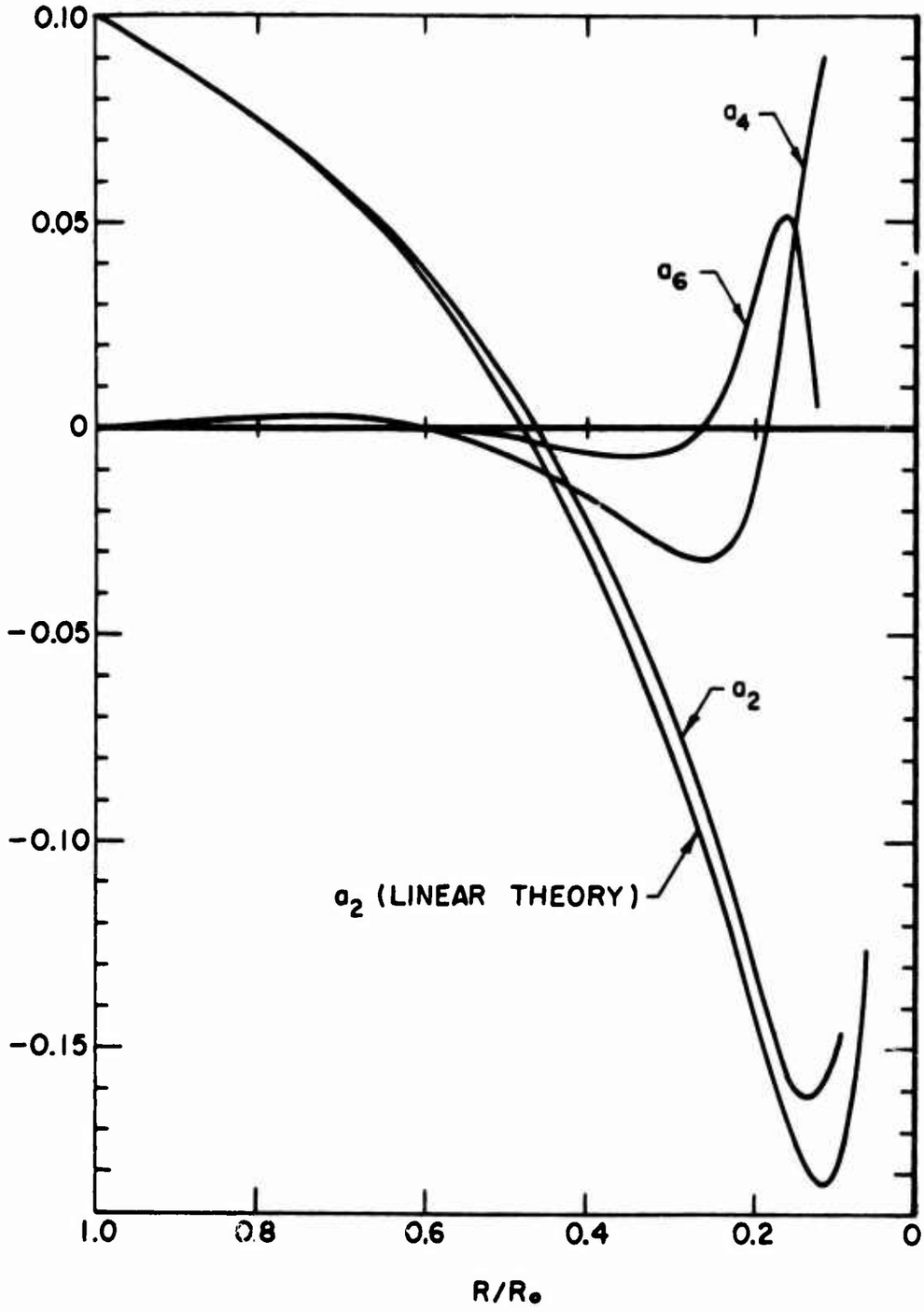

Fig. 3 Coefficients in Expansion of Bubble Radius for Case A.

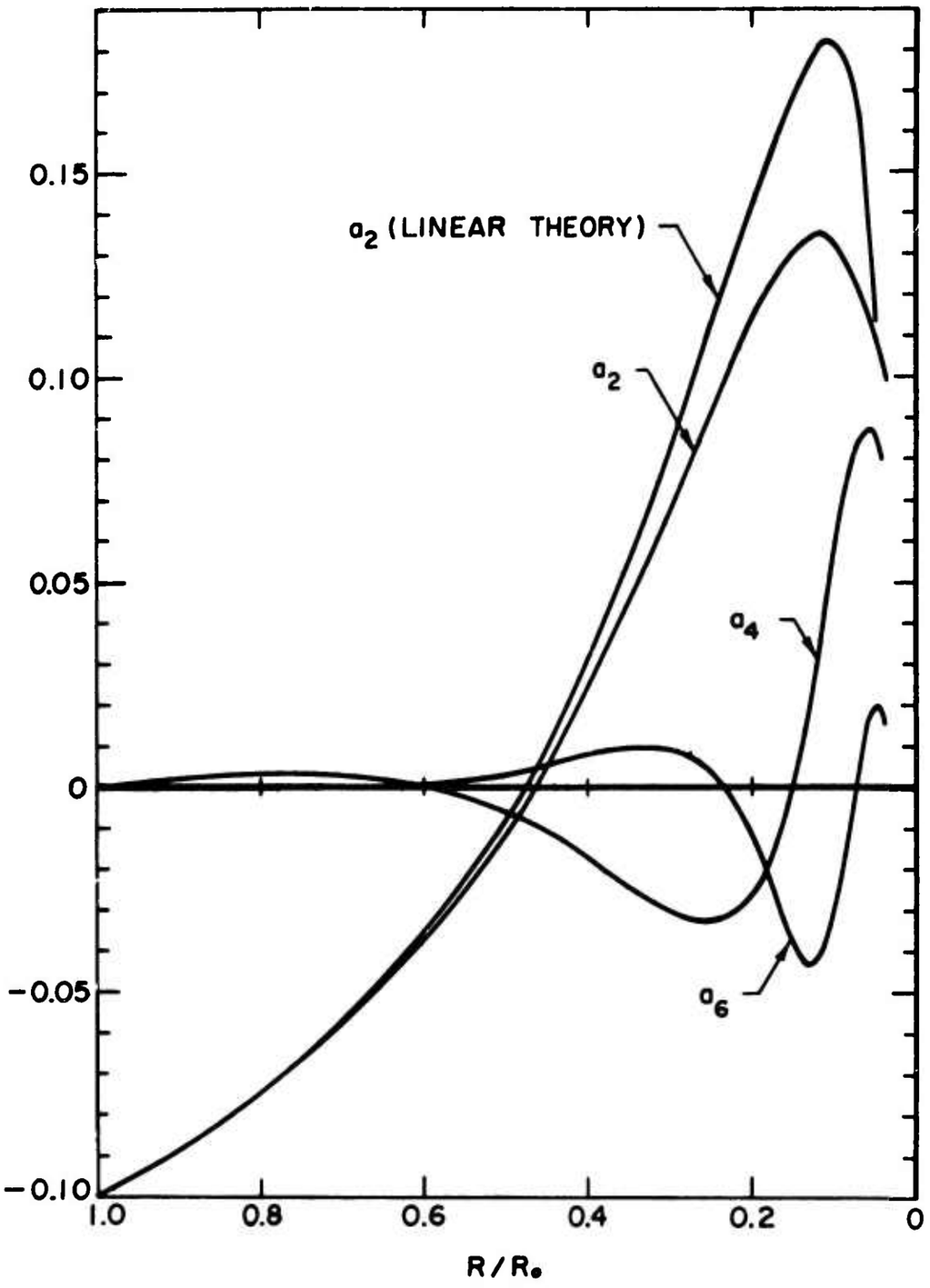

Fig. 4 Coefficients in Expansion of Bubble Radius for Case B.

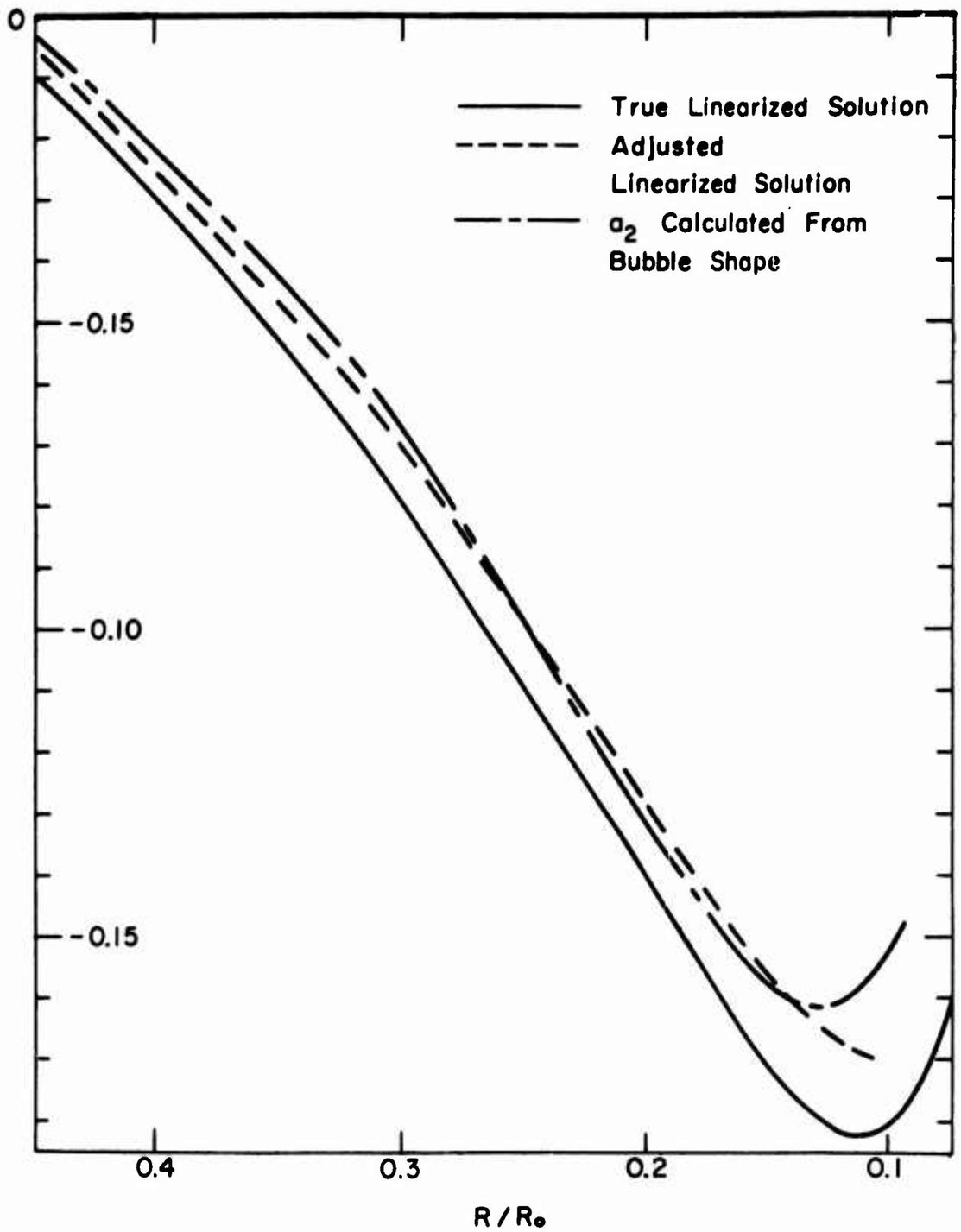

Fig. 5 Adjusted Linearized Solution Based on Finite Time Steps Used in Case A.

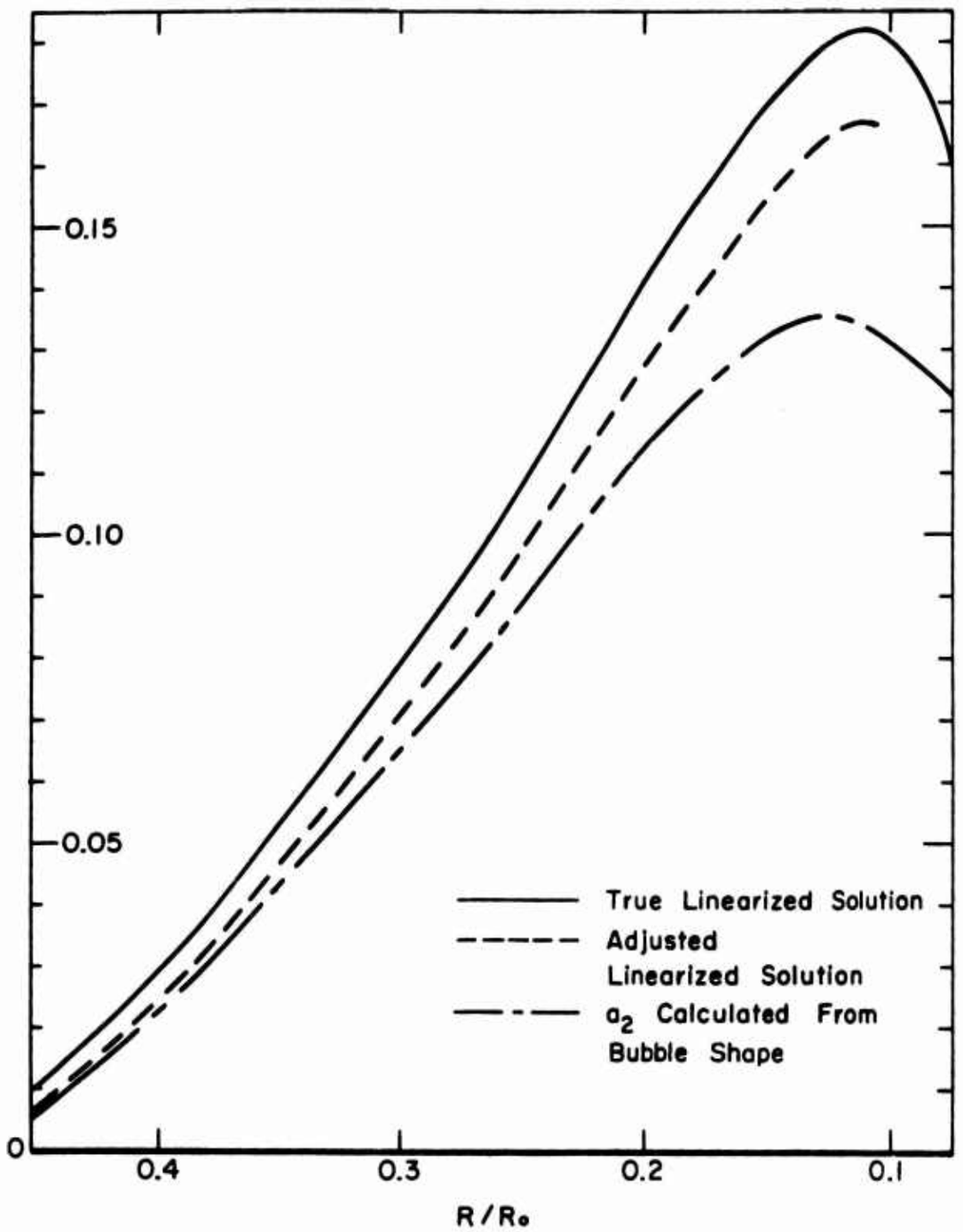

Fig. 6 Adjusted Linearized Solution Based on Finite Time Steps Used in Case B

Unclassified
Security Classification

DOCUMENT CONTROL DATA - R & D

(Security classification of title, body of abstract and indexing annotation must be entered when the overall report is classified)

1. ORIGINATING ACTIVITY (Corporate author)	2a. REPORT SECURITY CLASSIFICATION
California Institute of Technology Division of Engineering and Applied Science	X Unclassified
	2b. GROUP Not applicable

3. REPORT TITLE

NONLINEAR EFFECTS IN THE COLLAPSE OF A NEARLY SPHERICAL CAVITY IN A LIQUID

4. DESCRIPTIVE NOTES (Type of report and inclusive dates)

Technical report

5. AUTHOR(S) (First name, middle initial, last name)

Chapman, Richard B. and Plesset, Milton S.

6. REPORT DATE	7a. TOTAL NO. OF PAGES	7b. NO OF REFS
July 1970	9	4

8a. CONTRACT OR GRANT NO.	9a. ORIGINATOR'S REPORT NUMBER(S)
N00014-67-0094-0009	
b. PROJECT NO	Report No. 85-51
c.	9b. OTHER REPORT NO(S) (Any other numbers that may be assigned this report)
d.	

10. DISTRIBUTION STATEMENT

This document has been approved for public release and sale, its distribution in unlimited.

11. SUPPLEMENTARY NOTES	12. SPONSORING MILITARY ACTIVITY
	Office of Naval Research

13. ABSTRACT

A linearized perturbation theory was developed some time ago for the analysis of the growth of distortions in a nearly spherical cavity collapsing in a liquid. Since the distortions grow as the cavity collapses, it is of importance to determine the validity of the linearized approximation. The present study gives a numerical solution of the exact nonlinear equations for the growth of a distortion. Two kinds of distortions are studied in detail: Case A is essentially a prolate ellipsoid; Case B is essentially an oblique ellipsoid. Both cases have initial large deformations from the spherical shape. The numerical solution shows that the linearized perturbation approximation remains surprisingly accurate through most of the cavity collapse. The principle effect of the nonlinear calculation is in the coupling of the various distortion modes.

14. KEY WORDS	LINK A		LINK B		LINK C	
	ROLE	WT	ROLE	WT	ROLE	WT
Bubble collapse						
Nonlinear effects						